



FAULT DIAGNOSIS-BASED OBSERVERS USING KALMAN FILTERS AND LUENBERGER ESTIMATORS: APPLICATION TO THE PITCH SYSTEM FAULT ACTUATORS

Zakaria ZEMALI¹, Lakhmissi CHERROUN^{1,*} , Nadji HADROUG¹, Mohamed NADOUR¹, Ahmed HAFIFA^{1,2}

¹ Applied Automation and Industrial Diagnostics Laboratory, Faculty of Sciences and Technology, University of Djelfa, 17000 DZ, Algeria

² Department of Electrical and Electronics Engineering, Nisantasi University, 34398 Saryer, Istanbul, Turkey

* Corresponding author, e-mail: l.cherroun@univ-djelfa.dz

Abstract

This paper aims to present a robust fault diagnosis structure-based observers for actuator faults in the pitch part system of the wind turbine benchmark. In this work, two linear estimators have been proposed and investigated: the Kalman filter and the Luenberger estimator for observing the output states of the pitch system in order to generate the appropriate residual between the measured positions of blades and the estimated values. An inference step as a decision block is employed to decide the existence of faults in the process, and to classify the detected faults using a predetermined threshold defined by upper and lower limits. All actuator faults in the pitch system of the horizontal wind turbine benchmark are studied and investigated. The obtained simulation results show the ability of the proposed diagnosis system to determine effectively the occurred faults in the pitch system. Estimation of the output variables is effectively realized in both situations: without and with the occurrence of faults in the studied process. A comparison between the two used observers is demonstrated.

Keywords: Fault Detection, Estimation, Pitch System, Kalman Filter, Luenberger Observer.

List of Symbols/Acronyms

FDI – Fault Detection and Isolation;
 FTC – Fault-Tolerant Control;
 KF – Kalman Filter;
 LO – Luenberger Observer;
 RE – Relative Error;
 RMSE – Root Mean Square Error;
 WT – Wind Turbine;
 β_{ref} – Reference angle of the blade;
 β_m – Measured angle of the blade;
 ζ – Damping factor;
 ω_n – Natural frequency;
 $\dot{\beta}_i$ – Angular speed;
 β_r^i – Input vector;
 y_p^i – Measurable vector of output;
 $\tau_{g,r}$ – Torque generator reference;
 α_{gc} – Parameter model.

1. INTRODUCTION

In the last two decades, wind turbine (WT) presents an important renewable energy source for various electricity domains. Indeed, many applications and wind farms have been installed in the world to guarantee the continuous production of

electricity. The main principle of these machines is to generate electrical energy by transforming the kinetic energy of wind in the installed workspace, especially in areas where an important value of wind is founded.

Wind turbines operate for long periods of time, which increases their degradation rates and even the failure of various components such as: electronic control units, rotor blades, hydraulic parts, generators, sensors, and actuators) [1]. To guarantee continuous electrical production of energy, these faults must be avoided to reduce maintenance interventions and costs. Wind turbine systems have extremely employments and they are exposed externally for different environmental facts [1, 2]. The employed sensors and actuators in the wind turbines are affected by faults during operation such as faults in: gearbox, pitch system sensors and actuators, drive train parts, generator problems, sensors and actuators in the blades, converter problems [2, 3]. For this purpose, the condition-monitoring system must be designed and implemented as well as a performed structure for the used wind turbines.

In order to ensure the correct application and availability of wind turbine machines, different modern and intelligent techniques are employed and investigated to deal with this supervision system such as computational intelligence, real-time condition monitoring strategies, advanced diagnosis and control systems [1, 3, 4]. So, an instantaneous supervision and effective fault diagnosis system is needed to control the wind turbine in order to generate the appropriate energy by optimizing the power production with minimum mechanical vibrations and less occurred faults. Where, the main task is to detect and isolate the occurred faults in a short possible time [3, 5].

Different researches and studies have been proposed to deal with the diagnosis task of wind turbines using several approaches [3, 5-20]. These proposed methodologies adopt distinctive design of schemes, resulting in different properties according to the used techniques. They are based mainly on two mechanisms: model-based and data-based approaches [1, 3, 5]. However, the stability of the studied system is an important consideration for making them more conservative to achieve optimal performances [3].

Authors in paper [6], have proposed a Takagi-Sugeno fuzzy logic models to manage complicated and unknown situations of the wind turbine and to residual generators. Where the parameters of fuzzy models are estimated via a system identification strategy. Whereas, paper [7] based on the analysis of collected SCADA data sets, an artificial neural network is applied to identify faults in all components of the WT. A model-based approach for fault detection and isolation structure is employed to the wind turbine benchmark using T-S fuzzy logic system in paper [8]. Where, a robust fuzzy sliding mode observer is derived to generate the appropriate residuals corresponding the occurred faults. Authors [9] have investigated fault estimators using data-driven methodologies based on fuzzy models and neural networks. Two fault diagnosis solutions for condition monitoring of a wind turbine process are proposed and developed in this paper. In papers of Odgaard et al. [10 and 11], a total benchmark system of a specific kind of turbines is proposed and simulated. The mainly possible occurred faults are simulated with different scenarios in sensors, actuators, and system faults for all components of the horizontal three blades wind turbine: pitch system, the drive train, the generator, and the converting system. Paper [12], an effective fault diagnosis method is proposed for the previous WT model in [11]. Where, the elaborated structure is based on physical redundancy in sensors to carry out the correct residuals between all the process measurements. Then a crisp logic technique is used to classify actuator and sensor faults. Authors in [13], have presented a fault detection and isolation strategy for WT benchmark using a sliding mode observer for different faults. In the paper [14], an SVM method is combined with model-based

observer for detecting sensors and actuators faults in a wind turbine benchmark. In addition, authors in papers [15 and 16] have used a combined approach between Bayesian and set membership techniques for the design of fault diagnostic structure based on the FDI model. Authors in [17] have proposed a model-based FDI scheme as hybrid model based on adaptive thresholds varying on time in order to guarantee false-alarms for fault detection, approximation, and isolation estimator. Hence, paper [18] considered a Monte-Carlo method for the fault evaluation of sensors in a WT as a sensitivity analysis task. Deep learning algorithms are widely investigated due to their powerful performances for the fault diagnostic and prognosis of WT machine such as in papers [19, 20, 21, 22].

Fault diagnosis based observers are a very interesting methodology for dynamic systems [3, 23, 24, 25, 33]. It is a model-based fault detection approach, where the principal idea is to estimate and observe unmeasured variables and uncertainty parameters of the studied process [24]. Paper [26] presents an investigation of using artificial neural networks and Kalman filters for the detection of blade pitch system faults. Whereas, authors in [27] have proposed a Kalman filter to estimate the process parameters with an adaptive fuzzy inference system. Papers [25, 28] present adaptive fault-tolerant control (FTC) methodologies based observers for sensors and actuators under time-varying speeds for the wind turbine benchmark. Luenberger Observer also is an interesting estimator for linear systems [25], can be used for fault detection and diagnosis [24]. Such as in [29], where authors have designed an observer for electromechanical actuator. Whereas, paper [30] presents Luenberger Observer with a learning mechanism for an actuator fault detection based on fuzzy logic system. This proposed intelligent system is constructed under time-varying delays. Papers [31] investigate the design of Luenberger estimator for different multi-input and multi-output (MIMO) systems. Hence, authors in [32] present a comparison between some observers such as: Kalman filter, Luenberger estimator, sliding mode, and unknown input observer. A review on the recent fault tolerant control and diagnosis for WT is given in paper [3], including a set of state observers. Hence, other recent papers are focused on the investigation of fault detection and condition monitoring for the pitch system of a wind turbine machine using different processing schemes such as: SCADA data in [36], Extreme Random Forest optimized by Grey Wolf algorithm called (IGWO-ERF) in used paper [37], and a model based on Light Gradient Boosting Machine (LGBM) is proposed in paper [38].

The objective of this paper is to design and propose efficient fault diagnosis structure based observers using Linear Kalman filters and Luenberger estimators. The studied fault detection system is applied to failure detection in the pitch

system of an horizontal wind turbine benchmark. Actuator faults are studied and investigated in this paper.

For that, this paper is organized as: in section 2, the main parts of the wind turbine machine are described. A background of the employed observers is given in section 3. Section 4 will introduce and explain the proposed fault diagnosis structure using Kalman filter and Luenberger observers as output estimators. The obtained results for fault diagnosis are presented and discussed in section 5. Different tests are shown with a comparison study between the two elaborated observers. Whereas, section 6 will conclude this paper.

2. WIND TURBINE STRUCTURE

The WT that has been studied in this work is a horizontal turbine with three blades. This wind turbine machine is composed of a pitch system (aerodynamic part), a drive train as a mechanical part, and the electrical part as the generator with a converter (Fig. 1). Where the principal task is to convert the wind power as kinetic energy into electric energy. In this figure, we present an overview of the wind turbine benchmark model. The presented variables are given below as acronyms. To study and investigate a fault diagnosis approach, the used model must include the wind turbine sensors and actuators with their probable detected faults [10, 11]. The possible faults in the wind turbine must be efficiently detected and managed to avoid deterioration of the nominal operating conditions and become a critical issue hard to manage.

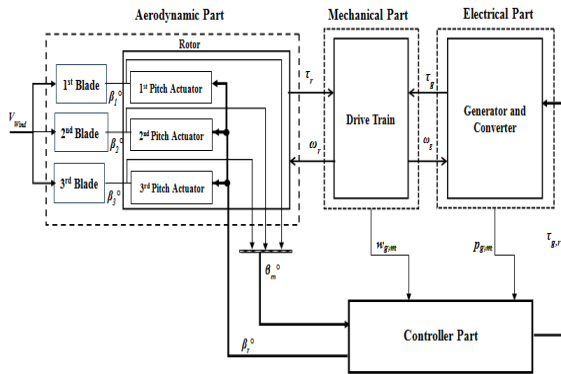


Fig. 1. Components of the wind turbine model

We can summarize each component as follows:

- **The pitch system:** is hydraulic piston servo where its function is to rotate the blade with an angle value denoted (β_m). This part of the WT machine is modelled with a second order closed-loop function [10] as presented in equation. 1. Where β_{ref} is the reference angle. It is a set point generated by the controller of the WT. However, β_m is the measured output used to adjust the pitch actuator system [11]. All blades of the wind turbine are identically modelled with the transfer function shown in eq. 1:

$$\frac{\beta_m}{\beta_{ref}} = \frac{\omega_n^2}{s^2 + 2\zeta\omega_n s + \omega_n^2} \quad (1)$$

β_{ref} : Reference angle of blade,

β_m : Measured angle value of the blade,

ζ : Damping factor equal to 0.6, ω_n : Natural frequency = 11.11 rad/s.

The state space of the pitch system can be written as follows:

$$\begin{aligned} \dot{x}_p^i &= \begin{bmatrix} -2\zeta\omega_n & -\omega_n^2 \\ 1 & 0 \end{bmatrix} x_p^i + \begin{bmatrix} 1 \\ 0 \end{bmatrix} \beta_r^i \\ y_p^i &= [0 \quad \omega_n^2] x_p^i \end{aligned} \quad (2)$$

Where: $x_p^i \begin{bmatrix} \hat{\beta}_i \\ \hat{\beta} \end{bmatrix}$ is the unmeasurable state of i -th

pitch angle, $\hat{\beta}_i$: is the angular speed, β_r^i : is the input vector, y_p^i : is the measurable vector of output.

We denote the matrices of the studied system as:

$$A_p = \begin{bmatrix} -2\zeta\omega_n & -\omega_n^2 \\ 1 & 0 \end{bmatrix}, B_p = \begin{bmatrix} 1 \\ 0 \end{bmatrix}, C_p = [0 \quad \omega_n^2] \quad (3)$$

The model of the blade and the pitch system is written as:

$$\begin{aligned} \dot{x}_p^i &= A_p x_p^i + B_p \beta_r^i, \\ y_p^i &= C_p x_p^i \end{aligned} \quad (4)$$

(A_p, B_p) are controllable, whereas, the matrixes (A_p, C_p) are observable.

- **Drive train:** is a mechanical part considered as a locomotive device. Its main role is to control the rotation speed of the rotor connected from the blades to the generator. The state space is given as:

$$\begin{bmatrix} \dot{\omega}_r(t) \\ \dot{\omega}_g(t) \\ \dot{\theta}_{\Delta}(t) \end{bmatrix} = A_{dt} \begin{bmatrix} \omega_r(t) \\ \omega_g(t) \\ \theta_{\Delta}(t) \end{bmatrix} + B_{dt} \begin{bmatrix} \tau_r(t) \\ \tau_g(t) \end{bmatrix} \quad (5)$$

The output of the state space is:

$$Y_{dt} = \begin{bmatrix} \omega_r(t) \\ \omega_g(t) \\ \theta_{\Delta}(t) \end{bmatrix} \quad (6)$$

- **Generator and Converter :**to generate electrical energy after converting it from mechanical energy [10]. It is modelled by a transfer function of first order such as:

$$\frac{\tau_g(s)}{\tau_{g,r}(s)} = \frac{\alpha_{gc}}{s + \alpha_{gc}} \quad (7)$$

$\tau_{g,r}$: torque generator reference, α_{gc} : is the parameter model of generator and converter. The function that represents the reproduced power by the generator is presented below in equation. 8, where

$\eta_g = 0.98$ represents the generator function efficiency.

$$p_g(t) = \eta_g \omega_g(t) \tau_g(t) \quad (8)$$

- **Controller:** The employed controller type is a proportional integrator (PI), and it works in two intervals for different wind speeds. Figure. 2 presents the operation modes of the wind turbine in different times. The controller works to protect the WT from damage during high wind speeds and to maintain the power generation to a reference value (4.8 MW) [11]. In the case when the speed is between [3-12.5 m/s] indicated in zone 2, it gives an action control to the generator in order to increase the energy to reach the required value, and when the speed become between [12.5-25m/s] as indicated in zone 3, the controller keeps the generator to produce energy continuously. The controller should switch between the two modes in the operating time.

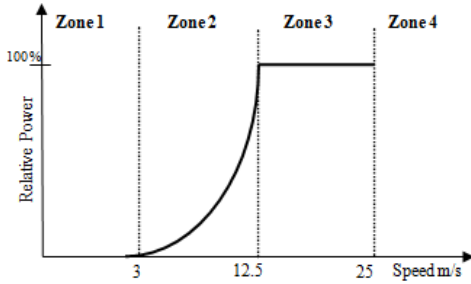


Fig. 2. Functioning modes of the WT controller

3. THE USED OBSERVERS

In this section, the used linear observers are presented which are Kalman Filter (KF) and Luenberger Observer (LO). A background of the two applied state estimators is given and demonstrated, especially for modeling and estimation of the pitch system outputs for horizontal wind turbine benchmark. Then, these observed values are employed to design effective and powerful fault detection and isolation systems.

3.1. Kalman Filter

The KF is a set of equations provides a computational recursive algorithm of estimation can be applied to dynamic systems. Kalman's Filter uses are many and in various areas [23, 24, 26]. It can also estimate the process state in all interval times. Among of them, the main characteristic is their robustness, and it isn't affected by perturbations [24, 32].

The principal structure of Kalman filter as estimator applied to linearized dynamic systems is shown in Fig. 3. To calculate the estimated value of the actual state of the process, we need only the current measurement and the estimated value from the previous time step. During estimation, the KF operates by propagating the mean and the covariance

of the state through the time[34]. The dynamic model as a state space of the observed system is written as:

$$\begin{cases} \dot{X}(t) = AX(t) + Bu(t) \\ Y(t) = CX(t) \end{cases} \quad (9)$$

Whereas, the algorithm calculation steps of KF are summarized as follows:

The predicted estimated state $\hat{X}_{k/k-1}$ as:

$$\hat{X}_{k/k-1} = A\hat{X}_{k-1/k-1} + Bu_k$$

The predicted estimated covariance $P_{k/k-1}$ as:

$$P_{k/k-1} = AP_{k-1/k-1} + A_Q^T + Q_k$$

The measured residues Y_k as :

$$\hat{Y}_k = Z_k - C\hat{X}_{k/k-1}$$

The innovation covariance S_k is given as:

$$S_k = CP_{k/k-1}C^T + R_k$$

The optimal Kalman gain K_k is then:

$$K_k = P_{k/k-1}C^T S_k^{-1}$$

A posteriori state estimated $\hat{X}_{k/k}$ can be

evaluated as follows: $\hat{X}_{k/k} = \hat{X}_{k/k-1} + K_k \hat{Y}_k$

Finally, the update estimated covariance $P_{k/k}$ is obtained: $P_{k/k} = (1 - K_k C)P_{k/k-1}$

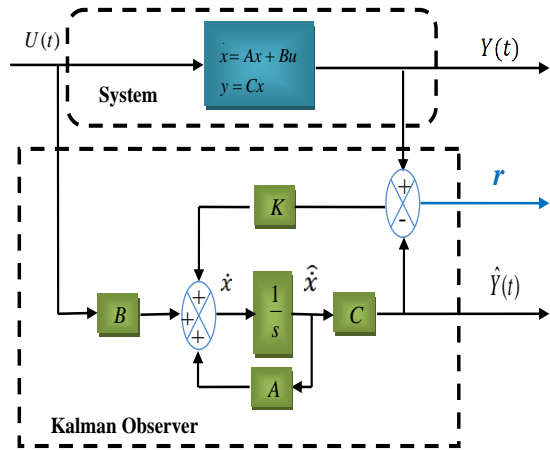


Fig. 3. Structure of estimation states using Kalman observer

3.2. Luenberger Observer

Luenberger observer is a deterministic estimator for linear systems, which can be only applied to state estimation of linear system with time-invariant property [30]. A simple and optimal solution is provided to the state estimation problem for multi-variable plants, where the objective of this observer is to generate the residuals in a system described by the following state space:

$$\begin{cases} \dot{X}(t) = AX(t) + Bu(t) \\ Y(t) = CX(t) \end{cases} \quad (10)$$

Figure. 3 presents the structure of estimation states using Luenberger observer. The relationship between the estimated process and the observer parameters is illustrated.

If the couple of (A, C) is completely observable, we can choose the values of the gain vector L such that the eigen values of the matrix defined by: (A-LC) [31, 32]. All of them have strictly negative real parts.

The state error (e) of the observer is calculated as follows:

$$e = x - \hat{x} \quad (11)$$

$$\dot{e} = \dot{x} - \dot{\hat{x}} = A(x - \hat{x}) + (Cx - C\hat{x}) \quad (12)$$

$$\begin{aligned} &= (Ax + Bu) - (A\hat{x} + Bu + L(Cx - C\hat{x})) \\ \dot{e} &= (A - LC)e \end{aligned}$$

The block observer state space of Luenberger can be written as:

$$\begin{cases} \frac{d\hat{x}}{dt} = A\hat{x} + Bu + L(Cx - C\hat{x}) \\ \hat{Y} = C\hat{x} \end{cases} \quad (13)$$

Where: $L \in \mathbb{R}^{2 \times 1}$: is the observer correction gain matrix

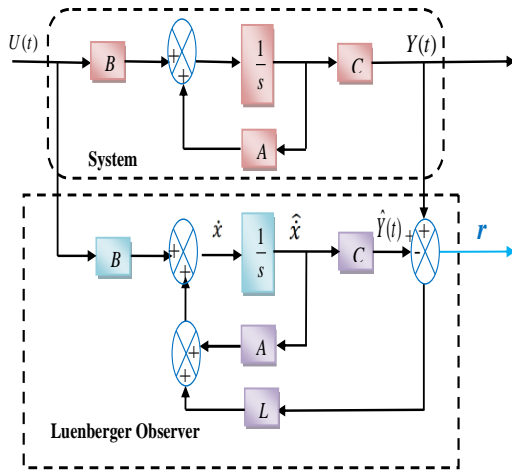


Fig. 4. Structure of estimation states using Luenberger observer

4. PROPOSED DIAGNOSIS STRATEGIES

Maintenance and operation costs of the WT system are significant for large-scale offshore types. So, an early detection and localization of defects is vital for maintaining availability with high degree and less costs of maintenance tasks.

In this section, we will present and discuss the elaborated fault diagnosis strategy based on Kalman and Luenberger observers. These two observers are used to defect detection task by estimating the system states using modelled data. Their advantages are relatively having low calculation cost, fast response, and a compact system representation for controlling the wind turbine benchmark. Observer's outputs are then compared with the WT sensor measurements to generate residuals. In normal

operating conditions (without faults or fault-free), the residual's is zero, and is changed under faulty conditions (occurrence of faults) when respecting all hypotheses of the designed observers.

The proposed structure is applied on the pitch system of the wind turbine. In this study, we have considered only the occurred major actuator faults in the pitch system. The overall structure of the proposed approach for fault diagnosis task is shown in Fig 5. Where the simulated wind turbine is based on the model of Odgaard [11], in which, the simulated faults are tested as impermissible deviation of the WT parameters from the nominal situation/value in the case of a faulty behaviour. This benchmark represents a WT with a nominal power of (4.8 MW) containing a three-blades and a controlled variable-speed.

The benchmark is used to simulate the proposed fault strategies on the pitch system actuators by changing the model parameters in equation. 1 as follows:

- Hydraulic pressure drop changes the parameters in the second pitch system to: $\zeta_2 = 0.45$ and $\omega_{n_2} = 5.73$.
- Increasing of air content changes the parameters in the third pitch system to: $\zeta_3 = 0.9$ and $\omega_{n_3} = 3.42$.

In this work, in order to test the effectiveness of the applied observers (KF and LO), we will study only the possible faults in the actuators of the pitch system denoted (β_2) and (β_3). These faults are a changing dynamic type. The tested faults are illustrated in table.1 using the third scenario of the benchmark model [11]. To investigate these faults, we have reconstructed the faulty system as a linear form according to equation. 1. The linear observers are direct methods to simplify the modelling of the dynamic system.

Table 1. Scenario of faults

Actuator Fault	Type	Symbol	Interval Time
F_1	Change	$\Delta\beta_2$	[2700s-2900s]
	Dynamic		[380s-3900s]
F_2	Change	$\Delta\beta_3$	[3400s-3500s]
	Dynamic		

The used observers: Kalman filter and Luenberger observer are used to estimate the unmeasured variables of the output (Y) for the pitch system denoted (\hat{Y}). In our case, the estimated value (\hat{Y}) is the position of the blades (β_2 , and β_3) for the both pitch positions, whereas, the actual outputs as measured variables are (β_{m_2} and β_{m_3}).

The dynamic model that can present the pitch system is defined in equation. 1 can be written using the state space as follows:

$$\begin{cases} \dot{X}(t) = AX(t) + Bu(t) \\ Y(t) = CX(t) \end{cases} \quad (14)$$

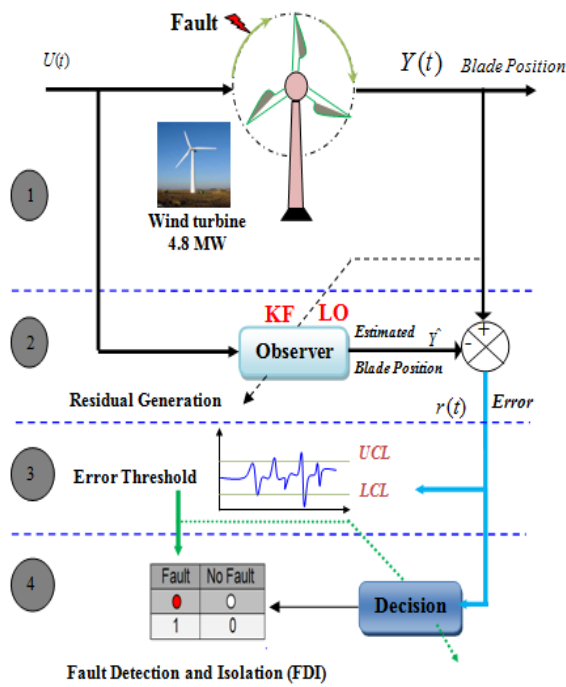


Fig. 5. Structure of the diagnosis strategy

The state space parameters of the pitch system model are as follows:

$$A = \begin{bmatrix} -13.3320 & -123.4321 \\ 1 & 0 \end{bmatrix}, B = \begin{bmatrix} 1 \\ 0 \end{bmatrix}, \\ C = [0 \quad 123.4321], D = [0] \quad (15)$$

Where: $X \in \mathcal{R}^{1 \times 2}$ is the state vector, $A \in \mathcal{R}^{2 \times 2}$: the system matrix, $B \in \mathcal{R}^{2 \times 1}$: the controllability matrix, $C \in \mathcal{R}^{1 \times 2}$: the observability matrix, $U = [\beta_r - \beta_{if}] \in \mathcal{R}^{1 \times 1}$: the input vector, and $Y = [\beta_m] \in \mathcal{R}^{1 \times 1}$ is the output vector.

To detect the possible occurred actuator faults in the pitch system, the proposed diagnosis structure using the two observers is based on four steps: Output Estimation, Residual Generation, Residual Evaluation, and Identification as follows:

1. Estimation using Observer: The purpose of using the Kalman filter and Luenberger observer as estimators is to approximate the output value of the system and discover the occurred fault in the studied plant. Each observer is designed in firstly to observe the actual output in healthy situations. In this step, the above estimation structures (Fig. 3 and Fig. 4) are used to determine the observers' parameters.

2. Residual generation: The residual is generated by comparing the output of the system and the output of the observer as shown in Fig. 5. Where the difference between the two outputs of the system and the model (observer) is considered as a residual. In this step, the residual r is calculated according to the responses of the process (pitch system) and the used estimator using the following equation at each time step.

$$r_{1,2} \in \mathcal{R}^{1 \times 1} = Y_{1,2} \in \mathcal{R}^{1 \times 1} - \hat{Y}_{1,2} \in \mathcal{R}^{1 \times 1} \quad (16)$$

Where: $Y(k)$ is the output of the pitch system, $\hat{Y}(k)$ is the observed output (KF or LO).

3. Residual Evaluation: After obtaining the residuals, a threshold with a fixed value is used from the value of the residuals. In this case, it is defined by two upper and lower values of thresholds denoted (UCL and LCL) for the residuals, because the residual has positive and negative values, for example $r_{1,2} \in [-0.5, 0.5]$. The goal is to determine the error field, so that when the signal exceeds the threshold, it is considered a fault, and if it does not exceed it, it is not considered a fault.

In this step a decision mechanism is applied to decide the existence of faults in the studied actuators.

So, two cases are considered:

- The residual value is between the interval $[-0.5; 0.5]$, $r = 0$, so: there isn't any fault.

- When the residual: $r_{1,2} \in [-1; -0.5] \cup [0.5; 1]$, so: $r = 1$, a fault is detected in the process.

4. Decision: to identify and locate the occurred faults, we have used a signature matrix to determine whether the faults studied have any relation with each other or not. In this case, we can see that the table is diagonal and the both faults are not related to each other as each fault happened at a different time and did not affect the second fault. In this step a decision mechanism is applied to decide the existence of faults in the studied actuators.

Table 2. Signature table

r	F_1	F_2
r_1	X	
r_2		X

5. RESULTS AND DISCUSSIONS

This section presents the obtained simulation results in order to demonstrate the ability and the efficiency of the proposed diagnosis structure. The suggested approach is verified on the horizontal WT benchmark measurements. Some tests and simulations comprising realistic faults in failure situations are illustrate the efficiency of the suggested methodology for detecting actuator faults in the pitch system. Based on the elaborated structure based observers that is presented in Fig. 5, the responses of the system and the detected faults are discussed here. We will present the obtained results for the two employed observers on two sub-sections: firstly, without faults, and secondly with the occurred faults in the actuators.

5.1. Results without faults using Kalman Filter (KF) and Luenberger Observer (LO)

In the case of operating the system without faults, Figures 6 to 9 present the positions of blades 2 and 3 denoted (β_2) and (β_3), and the generated residuals using the two proposed observers.

A. Blade Position Measurement (β_2)

Figures 6 (a) and 7(a) show the position measurements of blade 2 denoted (β_2) using the two observers: KF and LO respectively. Whereas Figures 6 (b) and 7(b) present the error as residuals

calculated between the process responses ($Y(t)$) and the estimated values $\hat{Y}(k)$ using the two observers as explained in eq. 22. In these figures, we present a zoom that shows the big similarity and the correct convergence between the two responses of the real system and the estimated values for the position of the blade 2 (β_2). It can be seen that in the case of normal functioning mode (without faults), the elaborated observers are able to estimate correctly the position variable, as depicted in the zoom captured in the interval time [2700s-2900s]. The pitch system actuator is working correctly without any problems, and the controlled system generates the desired (β_r) efficiently.

The error as residual is always zeros in all simulation time intervals which demonstrates the efficiency of the estimation used step.

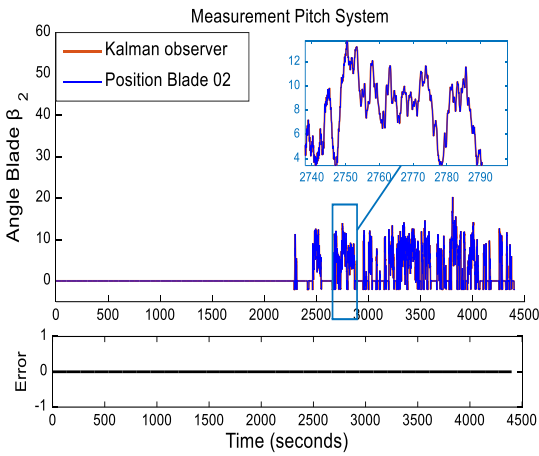


Fig. 6. Position of the second blade (β_2) and the Residual (using KF)

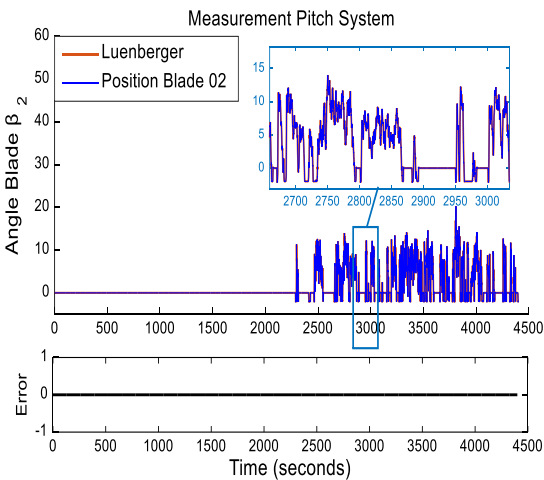


Fig. 7. Position of the second blade (β_2) and the Residual (using LO)

B. Blade Position Measurement (β_3)

With the same manner as previously, Figures 8 (a) and 9(a) presents observes values of the angle variable for the blade 3 denoted (β_3). For each used observer, the generated error as residual is shown in Figures 8(b) and 9(b). As can be seen, residuals are zeros which demonstrate the capability of the designed observers (Kalman Filter and Luenberger

observer) to estimate correctly the position variable of blade 3. A zoom part for each observer is illustrated in the time interval [3400s-3600s]. The studied actuator (β_3) of the pitch system works correctly and the blade rotates efficiently according the desired angle generated from the controller as a reference.

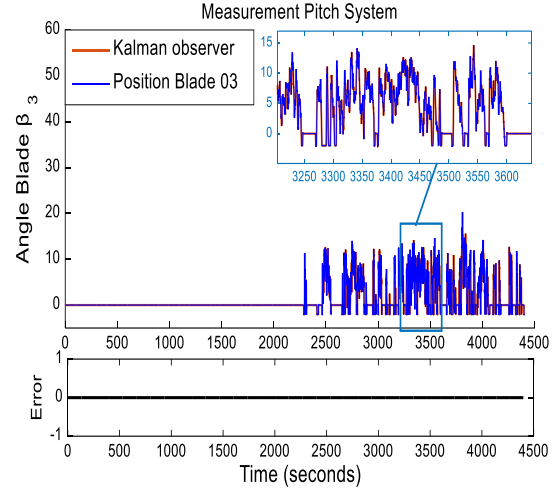


Fig. 8. Position of the third blade (β_3) and the Residual (using KF)

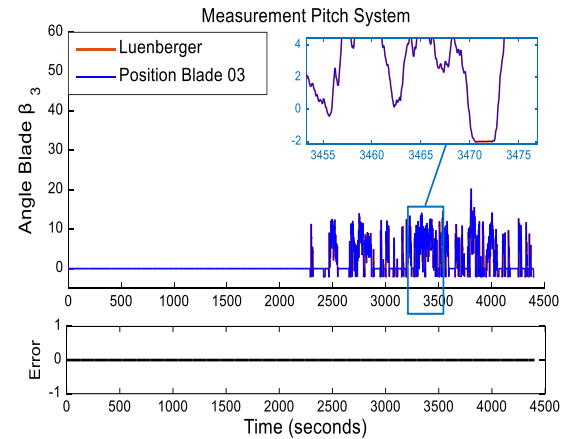


Fig. 9. Position of the third blade (β_3) and the Residual (using LO)

5.2. Results with Fault Occurrence in (β_2) and (β_3)

A. Using Kalman Filter

In the case of occurred faults in the actuators of the pitch system in the studied wind turbine. The results are depicted in Figures 10 and 11 respectively for the two blade actuators using Kalman filter.

The first fault is simulated as a dynamic change, pump problems or leakage, and a slow control action. Using the benchmark model presented previously with the fault scenarios, this fault can be expressed by changing the parameters: ξ and ω_n in (equation. 1) with the following values: $\xi_2 = 0.45$ and $\omega_{n2} = 5.73$.

Fig. 10(a) shows the responses of the angle of the pitch system 2 denoted (β_2) which is considered as a real output ($Y(t)$), and the estimated one by the Kalman observer denoted ($\hat{Y}(t)$). In the captured zoom of these two responses, we can see a difference between the two curves in a time interval corresponding the period of occurring a fault in the studied system. The generated residual as error between the position of the blade with the estimated values ($Y(t)$ and $\hat{Y}(t)$) is depicted in Fig. 10(b) demonstrating the occurrence of fault in the time interval [2700s-2900s]. It expresses a variation between the two responses. The area between the two intermittent lines represents the upper and lower threshold. It is determined experimentally on the studied process.

Whereas, Fig. 10(c) shows the detection and isolation of the fault that happened in the second pitch system (β_2) during (200s) and exactly in the interval time [2700s-2900s]. This fault is denoted (F_1).

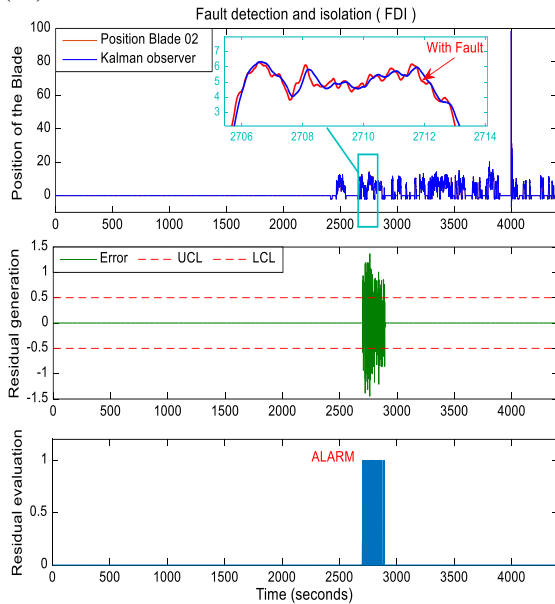


Fig. 10. The position of blade 2 (β_2) with fault, (b) Residual, (c) detection of the first actuator fault

For the second actuator fault, the simulation parameter is: $\xi_3 = 0.9$ and $\omega_{n2} = 3.42$, where they represent a change dynamics as Air in oil, a slow control action.

Figure. 11(a) shows the two responses of the system and the KF as observer for (β_3) respectively. The variation of the dynamic system parameters evolves a difference between the measured outputs. In the interval [3400s - 3500s], an error is observed as depicted in Fig. 11(b) illustrates the detection of the occurred fault in the system.

Fig. 11(c) shows the detected fault that has been occurred in the third pitch system (β_3) during (100s) in the interval [3400s - 3500s].

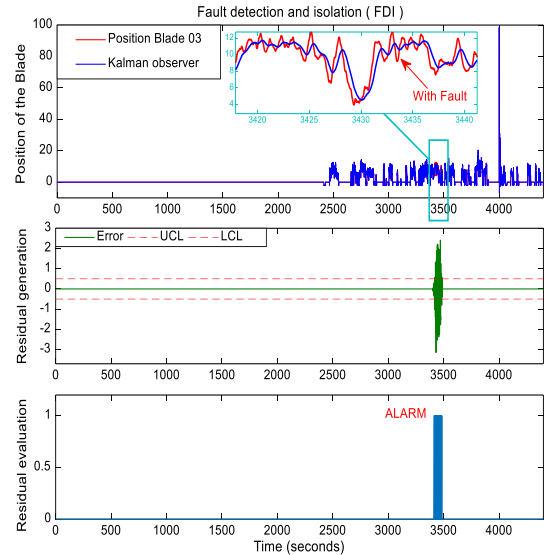


Fig. 11. The position of blade 3 (β_3) with fault, (b) Residual, (c) detection of the actuator fault

B. Using Luenberger Observer

With the occurred of faults in the actuators of the pitch system, the obtained results using Luenberger observer are shown in Figures 12 and 13 respectively for the two blade actuators. We have used the same simulation parameters of the system and the faults. Where, the fault is simulated as a dynamic change with the same parameters of the transfer function ξ and ω_n .

Firstly, Fig. 12(a) shows the two responses of the angle of the pitch system 2 (β_2). In which, $Y(t)$ is the real output of the studied wind turbine part, and $\hat{Y}(t)$ is the estimated measurement using the designed Luenberger observer. In the captured zoom of these two responses, we can see a difference between the two curves. This is demonstrated in Fig. 12(b) demonstrating the generated residual of the position of the blade with fault occurrence. The residual is captured in an interval time of [3400s-3500s], where it expresses a variation between the two responses according to the applied fault. This error is measured over the upper and lower threshold limits.

Using the proposed diagnosis strategy, the occurred fault can be detected correctly in the corresponding time interval as shown in Fig. 12(c). The occurred fault (F_2) in the third pitch system (β_3) during (100s) in the interval time [3400s-3500s].

The responses of the simulated test with second actuator fault (F_2) are depicted in Figure. 13(a, b and c). Where, Figure. 13(a) presents the two responses of the system and the observer ($Y(t)$ and $\hat{Y}(t)$) respectively. The variation of the dynamic system parameters evolves a difference between the measured outputs. In the interval [3400s-3500s], an error is observed as depicted in Fig. 13(b) illustrates the detection of the occurred fault in the system. The occurred fault in the third pitch system (β_3) is detected during a period of (100s) in the interval time of operation [3400s-3500s].

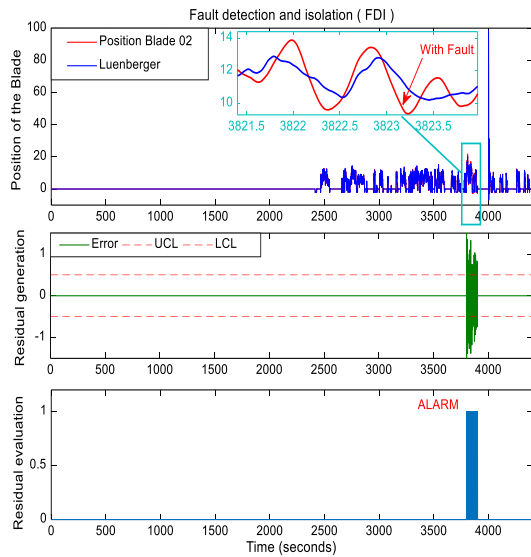


Fig. 12. The position (β_2) with fault, (b) Residual, (c) detection of the second actuator fault

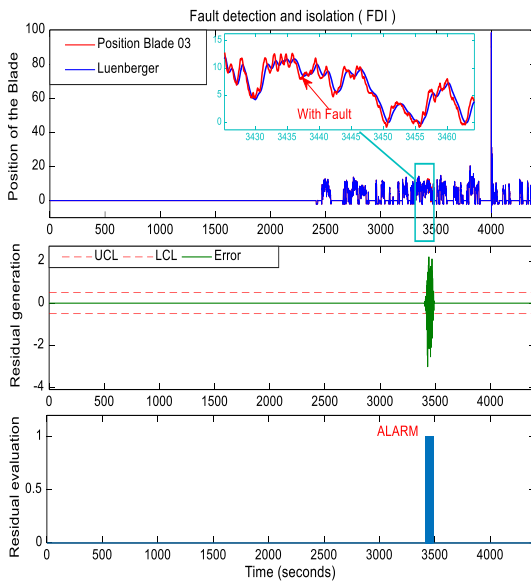


Fig. 13. The position of blade 3 (β_3) with fault, (b) Residual, (c) detection of the actuator fault

According to these obtained results obtained, we can approve that the proposed fault diagnosis strategy is well performed using the two designed observers: Kalman filter and Luenberger estimator. The behaviour of the studied wind turbine part is modelled correctly, in which the output variables are estimated with a minimum of errors. Based on this estimation step, the overall diagnosis system can generate the appropriated residual corresponding to the occurred faults in the pitch system using the two observers (KF and LO). Then the decision step makes precisely the correct classification of faults.

The proposed diagnosis structure is very adapted and attractive to ensure the optimal productivity of the wind turbine.

C. Comparison between KF and LO

To show the ability of the estimation process, and the effectiveness of the proposed fault diagnosis based observers, in this section, the responses of the pitch system using the two elaborated observers are illustrated simultaneously in the case of a faulty system. Figures 14 and 15 present the position of the second and the third blade respectively with their generated residuals in the case of occurrence of actuator faults (F_1) and (F_2).

In order to determine which observer is better for estimating the output values of the pitch system, we have used two indicators of comparisons as a function of confidence indices.

The first is the relative normal error denoted (RE). It is used to measure the estimation precision by using the following equation:

$$RE = \frac{\|Y - Y_s\|}{\|Y\|} \quad (17)$$

The second indicator is the Root Mean Square Error (RMSE). It is used for measuring the ability of data prediction and defined by:

$$RMSE = \sqrt{\frac{\sum_{i=1}^n (Y - \hat{Y})^2}{n}} \quad (18)$$

Where:

- Y : the measured blade position (β_2 or β_3),
- \hat{Y} : the estimated value using the observers.
- n : number of points (measurements).

Based on the applied confidence and rating indices RE and RMSE, Table 3 presents a summary of the calculated values as a comparison between the two used observers (KF and LO) for the pitch system prediction. The simulated faults in the position of blades are investigated. The applied Kalman filter and Luenberger observers are stochastic estimators for linear systems. To estimate effectively the process outputs, the KF is based on correction matrix to define the gain parameters, whereas, the LO employs the pole placement.

As can be seen in the Figures (14(a) and 15(a)) of the position blades using the two designed observers compared to the measured one of the studied system, the two estimators behave correctly for the wind turbine part (pitch system). From the presented simulation results in Fig. 14(b), the calculated residual in KF is less than LO depending to the proposed poles and the gain matrix (L) that has been calculated. This may give a small difference in the residual generated between the two responses.

The effectiveness of each estimator is compared according to the fault detection response in the interval of occurrence. The range variation of the residual using LO is the least one while comparing with KF residual, which is the highest. But the applied failure is detected and localized effectively in the two cases: fault in (β_2) is detected during a period of (100s) in the interval time [3800s-3900s] (as in Fig. 14(b), and the fault in (β_3) is detected in the interval time of operation [3400s-3500s] (as in Fig. 15(b)).

Table 3. Comparison between KF and LO for the pitch system prediction

	Second Blade (β_2)		Third Blade (β_3)	
	Luenberger Observer (LO)	Kalman Observer (KO)	Luenberger Observer (LO)	Kalman Observer (KO)
RE	0.8804	0.9215	0.8802	0.9212
RMSE	45.0333	45.8712	45.0796	45.9203
Best Observer	> Luenberger Observer		> Luenberger Observer	

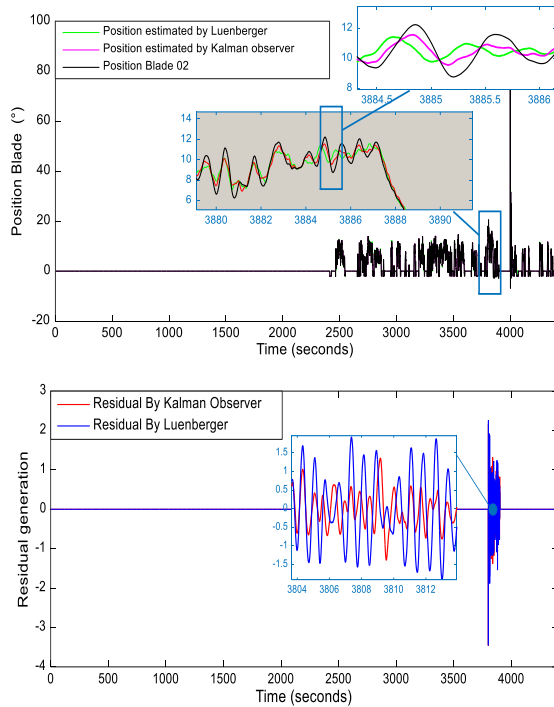


Fig. 14. (a) Position of the second blade, (b) Generated residual

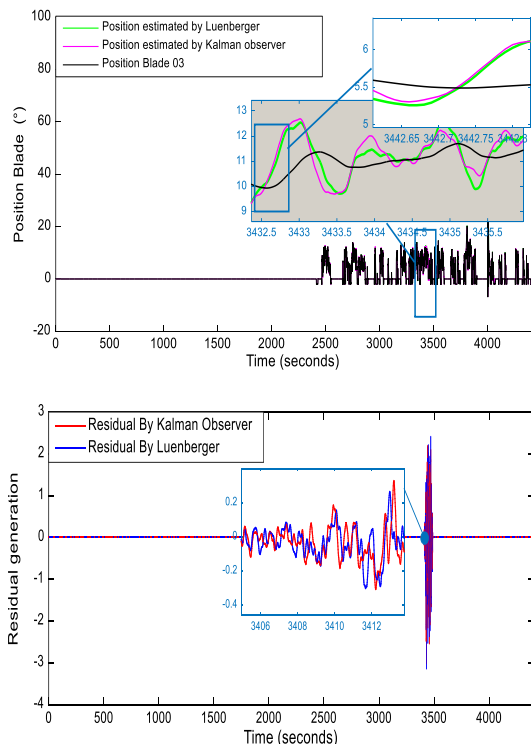


Fig. 15. (a) Position of the third blade, (b) Generated residual

6. CONCLUSION

In this paper, an efficient fault diagnosis structure based observers is proposed using Kalman filter and Luenberger observer for the pitch angle system with three-blades horizontal-axis WT. Actuator faults have been investigated and detected using this fault detection strategy. The proposed defect detection with isolation system is based on the observation of the output values using the elaborated observers in order to generate the corresponding residual of the occurred fault. A threshold value is defined in the decision step to detect faults correctly after estimation of the output variables. The KF and LO are designed in such a way that faults are considered as exogenous output disturbances to be rejected, which provides an accurate/fault-free state estimation. A comparison study is shown between the two designed observers to show characteristics of each one using some performance indices and results. All simulated actuator faults are detected and identified successfully in the pitch angle system.

As perspectives, simulation of all faults in the rest parts of the WT machine such as the drive train and the generator with its converter. An equivalent model using intelligent techniques may define correctly the behaviour of the studied pitch system.

Author contributions: *research concept and design, Z.Z., L.C.; Collection and assembly of data, Z.Z., N.H.; Data analysis and interpretation, L.C., M.N.; Writing the article, Z.Z., L.C., N. H., M.N.; Critical revision of the article, L.C., M.N., A.H.; Final approval of the article, L.C., A.H.*

Declaration of competing interest: *The authors declare that they have no known competing financial interests or personal relationships that could have appeared to influence the work reported in this paper.*

REFERENCES

- Gao Z, Liu X. An Overview on fault diagnosis, prognosis and resilient control for wind turbine systems. *Processes*. 2021;9:300. <https://doi.org/10.3390/pr9020300>.
- Stetco A, Dinmohammadi F, Zhao X, Robu V, Flynn D, Barnes M, Keane, J, Nenadic G. Machine learning methods for wind turbine condition monitoring: A review. *Renew Energy*. 2019;133:620–635. <https://doi.org/10.1016/j.renene.2018.10.047>
- Fekik A, Habibi H, Simani S. Fault diagnosis and fault tolerant control of wind turbines: An overview. *Energies*. 2022;15:7186. <https://doi.org/10.3390/en15197186>.
- Zhu Y, Zhu C, Tan J, Song C, Chen D, Zheng J. Fault detection of offshore wind turbine gearboxes based on deep adaptive networks via considering Spatio-temporal fusion. *Renewable Energy*. 2022;200:1023–1036. <https://doi.org/10.1016/j.renene.2022.10.018>
- Pandit R, Astolfi D, Hong J, Infield D, Santos M. SCADA data for wind turbine data-driven condition/performance monitoring: A review on state-of-art, challenges and future trends, *Wind*

- Engineering. 2022;1-20.
<http://doi:10.1177/0309524X221124031>.
6. Simani S, Farsoni P, Castaldi P. Wind turbine simulator fault diagnosis via fuzzy modelling and identification techniques. *Sustainable Energy, Grids and Networks*. 2015;1:45–52
<http://dx.doi.org/10.1016/j.segan.2014.12.001>
 7. Zhang Z, Wang K. Wind turbine fault detection based on SCADA data analysis using ANN. *Advance Manuf.* 2014;2:70–78. <http://doi:10.1007/s40436-014-0061-6>
 8. Simani S, Castaldi P. Intelligent fault diagnosis techniques applied to an offshore wind turbine system. *Appl. Sci.* 2019;9:783.
<https://doi:10.3390/app9040783>
 9. Zhu H, Liu J, Zhu H, Lu D, Wang Z. A novel wind turbine fault detection method based on fuzzy logic system using neural network construction method. *IEEE International Conference on Industrial Application of Artificial Intelligence, IAAI, 2021*.
<https://doi.org/10.1016/j.ifacol.2021.04.157>
 10. Odgaard PF, Stoustrup J, Kinnaert M. Fault tolerant control of wind turbines- a benchmark model. 7th IFAC symposium on fault detection, supervision and safety of technical processes. 2009:155-160.
<https://doi.org/10.3182/20120829-3-MX-2028.00185>
 11. Odgaard PF, Stoustrup J, Kinnaert M. Fault-tolerant control of wind turbines: A benchmark model. *IEEE Transactions on Control Systems Technology*. 2013;21(4):1168–1182.
<https://doi.org/10.3182/20090630-4-ES-2003.00026>
 12. Saci A, Cherroun L, Hafaifa A, Mansour O. Effective fault diagnosis method for the pitch system, drive train and the generator with converter in a wind turbine system. *Electrical Engineering*. 2022;104(4):1967-1983. <https://doi.org/10.1007/s00202-021-01446-8>.
 13. Borja-Jaimes V, Adam-Medina M, López-Zapata BY, Valdés LG, Pachecano LC, Coronado ME. Sliding mode observer-based fault detection and isolation approach for a wind turbine benchmark. *Processes*. 2022;10:54. <https://doi:10.3390/pr10010054>
 14. Laouti N, Othman S, Alamir M, Othman NS. Combination of model-based observer and support vector machines for fault detection of wind turbines. *International Journal of Automation and Computing*. 2014;11:274-287. <https://doi.org/10.1007/s11633-014-0790-9>
 15. Fernandez-Canti RM, Blesa J, Tornil-Sin S, Puig V. Fault detection and isolation for a wind turbine benchmark using a mixed Bayesian/Set-membership approach. *Annual Rev. in Control*. 2015;40:59-69.
<https://doi.org/10.1016/j.arcontrol.2015.08.002>
 16. Kościelny JM, Bartyś M, Szytby A. Diagnosing with a hybrid fuzzy–Bayesian inference approach, *Engineering Applications of Artificial Intelligence*. 2021;104:104345.
<https://doi.org/10.1016/j.engappai.2021.104345>
 17. Liu Y, Ferrari R, Wu P, Jiang X, Li S, Wingerden JW. Fault diagnosis of the 10mw floating offshore wind turbine benchmark: a mixed model and signal-based approach. *Renew. Energy*. 2021;164:391-406.
<https://doi.org/10.1016/j.renene.2020.06.130>
 18. Biazar D, Khaloozadeh H, Siah M. Sensitivity analysis for evaluation of the effect of sensors error on the wind turbine variables using Monte Carlo simulation. *IET Renew. Power Gener.* 2022;16:1623–1635. <https://doi.org/10.1049/rpg2.12468>
 19. Wang Z, Gao SL, Yao L, Qi X, Zhang J. Data-driven fault diagnosis for wind turbines using modified multiscale fluctuation dispersion entropy and cosine pairwise-constrained supervised manifold mapping. *Knowledge-Based Systems*. 2021;228:107276.
<https://doi.org/10.1016/j.knsys.2021.107276>
 20. Li Y, Jiang W, Zhang G, Shu L. Wind turbine fault diagnosis based on transfer learning and convolutional autoencoder with small-scale data. *Renewable Energy*. 2021;171:103-115.
<https://doi.org/10.1016/j.renene.2021.01.143>
 21. Chen W, Qiu Y, Feng Y, Li Y, Kusiak A. Diagnosis of wind turbine faults with transfer learning algorithms, *Renewable Energy*. 2021;163:2053-2067.
<https://doi.org/10.1016/j.renene.2020.10.121>
 22. Chang Y, Chen J, Qu C, Pan T, et al. Intelligent fault diagnosis of wind turbines via a deep learning network using parallel convolution layers with multi-scale kernels. *Renewable Energy*. 2020;153:205-213.
<https://doi.org/10.1016/j.renene.2020.02.004>.
 23. Zemali Z, Cherroun L, Hafaifa A, Hadroug N. Fault diagnosis structure based on Kalman filter for the pitch system of a wind turbine process. 2nd Algerian Symposium on Renewable Energy and Materials ASREM2022. 2022.
 24. Teng J, Li C, Feng Y, Yang T, Zhou R, Sheng Z. adaptive observer based fault tolerant control for sensor and actuator faults in wind turbines. *Sensors*. 2021;21: 8170. <https://doi.org/10.3390/s21248170>.
 25. Jlassi J, et al., Multiple open-circuit faults diagnosis in back-to-back converters of PMSG drives for wind turbine systems. *IEEE Transactions on Power Electronics*. 2015;30(5).
<https://doi:10.1109/TPEL.2014.2342506>
 26. Cho S; Choi M, Gao Z, Moan T. Fault detection and diagnosis of a blade pitch system in a Floating Wind Turbine based on Kalman Filters and Artificial Neural Networks. *Renew. Energy*. 2021;169:1-13.
<https://doi.org/10.1016/j.renene.2020.12.116>
 27. Kim D, Lee D. Fault parameter estimation using adaptive fuzzy fading Kalman filter. *Applied Sciences*. 2019;9:3329. <http://doi:10.3390/app9163329>.
 28. Ye M, Zhang J, Yang J. Bearing fault diagnosis under time-varying speed and load conditions via observer-based load torque analysis. *Energies*. 2022;15:3532.
<https://doi.org/10.3390/en15103532>
 29. Horváth Z, Molnárka G. Design Luenberger observer for an Electromechanical Actuator, *Acta Technica Jaurinensis*. 2014;7(4):328-343.
<https://doi:10.14513/actatechjaur.v7.n4.313>.
 30. Jia Q, Wu L, Li H. Robust actuator fault reconstruction for Takagi-Sugeno fuzzy systems with time-varying delays via a synthesized learning and Luenberger observer. *International J. of Control, Automation and Systems*. 2021;9(2):799-809.
<http://dx.doi.org/10.1007/s12555-019-0747-4>.
 31. Ortega R, Praly L, Aranovskiy S, Yi B, Zhang. On dynamic regressor extension and mixing parameter estimators: Two Luenberger observers interpretations. *Automatica*. 2018;95:548–551.
<https://doi.org/10.1016/j.automatica.2018.06.011>
 32. Kumar V, Jerome EK, Ayyappan S. Comparison of four state observer design algorithms for MIMO system,. *Archives of Control Sciences*. 2013;23(LIX):131-144. <https://doi.org/10.2478/acsc-2013-0015>
 33. Boutat D, Zheng G. Observer design for nonlinear dynamical systems, lecture notes in control and information sciences. Springer Cham. 2021:487.
<https://doi.org/10.1007/978-3-030-73742-9>

34. Nail B, Kouzou A, Hafaifa A, Hadroug N, Puig V. A robust fault diagnosis and forecasting approach based on Kalman filter and interval type-2 fuzzy logic for efficiency improvement of centrifugal gas compressor system. *Diagnostyka*. 2019;20(2):57-75. <https://doi.org/10.29354/diag/108613>
35. Ben Djoudi H.CH, Hafaifa A, Djoudi D, Guemana M. Fault tolerant control of wind turbine via identified fuzzy models prototypes, *Diagnostyka*. 2020; 21(3): 3-13. <https://doi.org/10.29354/diag/123220>
36. McKinnon C; Carroll J, McDonald A, Koukoura S, Plumley C. Investigation of isolation forest for wind turbine pitch system condition monitoring using SCADA data. *Energies*. 2021;14:6601. <https://doi: 10.3390/en14206601>
37. Tang M, Yi J, Wu H, Wang Z. Fault detection of wind turbine electric pitch system based on IGWO-ERF. *Sensors* 2021;21:6215. <https://doi: 10.3390/s21186215>.
38. Tang M, Peng Z, Wu H. Fault detection for pitch system of wind turbine-driven doubly fed based on IHHO-LightGBM. *Appl. Sci.* 2021;11:8030. <https://doi: 10.3390/app11178030>

Received 2022-12-11
Accepted 2023-02-16
Available online 2023-02-17



Zakaria ZEMALI was born in Djelfa Algeria on 28/08/1992. He obtained the License and Master degrees at 2014 and 2016 respectively in Electrical Engineering, option: Maintenance of Industrial Instrumentation from Faculty of Sciences and

Technology, University of Djelfa, Algeria. Now he is a PhD student on Instrumentation, and a member of the Applied Automation and Industrial Diagnostics Laboratory. His interest includes: fault diagnosis techniques and prognostic for wind turbine systems.

E-mail address: z.zemali@univ-djelfa.dz



Lakhmissi CHERROUN received the state engineer degree in 2006, the magister in 2009 and the Phd degree in 2014, all in automatic and control from the department of automatic, university of Biskra, Algeria. He is currently an associate professor at Electrical

Engineering department, university of Djelfa, Algeria. He is the head of the Modeling, Identification and Control of Dynamic Systems Research Team, LAADI laboratory, University of Djelfa. His research interests include: robotics, intelligent systems and fault diagnosis techniques.

E-mail address: l.cherroun@univ-djelfa.dz



Nadji HADROUG was born on 18/12/1989 in Hassi Bahbah, Djelfa, Algeria. He is a member of the Applied Automation and industrial diagnostics laboratory, university Djelfa. His main researches are on the NeuroFuzzy fault tolerant control applied on a gas turbine. His thesis focuses on the development of new methods and tools in control fault tolerant for industrial systems. He is author and co-author of several publications and conference papers.

E-mail address: n.hadroug@univ-djelfa.dz



Mohamed NADOUR received the state engineer degree in 2006 in communication from university of Laghouat-Algeria, the magister degree in 2010 in advanced techniques in signal processing from Polytechnic Military school (EMP)-Algiers.

He obtained the PhD degree in automatic and control at university of Biskra in 2020. He is currently an associate associate professor at Electrical Engineering department, university of Djelfa. His research interests include: control, robotics and diagnostics.

E-mail address: m.nadour@univ-djelfa.dz



Ahmed HAFAlFA was born in Algeria in 1974. He received the State Engineer degree in 2000 on Applied Automation, the Magister degree in 2004 on Applied Automation and control systems and the PhD on Applied Automation and

Signal Processing in 2010 from the UMBB Boumerdes University. He received the Habilitation from the University of Sciences and Technology Houari Boumediene - USTHB - Faculty of Electronics and Computer Science, Department of Instrumentation and Automation on 2012. He is a PhD and Full Professor in Industrial Process: Automation / Diagnosis and Reliability Engineering at the Science and Technology Faculty of the University of Djelfa, Algeria, where he is pursuing his researches as a researcher at the Applied Automation and Industrial Diagnostic Laboratory of the University of Djelfa. Professor Ahmed HAFAlFA has participated in several international research projects and has led several national research projects. Currently he is the Director of the Applied Automation and Industrial Diagnostic

Laboratory of the University of Djelfa. His research area of interests includes the modelling and control in industrial systems, the diagnosis and new reliability engineering, fault detection and isolation in industrial process, intelligent system based on fuzzy logic and neural networks.

E-mail address: a.hafaifa@univ-djelfa.dz.

ahmed.hafaifa@nisantasi.edu.tr